Available online at www.sciencedirect.com
SCIENCE DIRECT
Journal of Power Sources 157 (2006) 666–673
JOURNAL OF POWER SOURCES
www.elsevier.com/locate/jpowsour

Portable proton exchange membrane fuel-cell systems for outdoor applications

M. Oszcipok *, M. Zedda, J. Hesselmann, M. Huppmann, M. Wodrich, M. Junghardt, C. Hebling

Fraunhofer Institute for Solar Energy Systems, Germany

Received 10 October 2005; accepted 2 January 2006
Available online 24 February 2006

Abstract

A hydrogen fuelled, 30 W proton exchange membrane fuel-cell (PEMFC) system is presented that is able to operate at an ambient temperature between −20 and 40 °C. The system, which comprises the fuel-cell stack, pumps, humidifier, valves and blowers is fully characterized in a climatic chamber under various ambient temperatures. Successful cold start-up and stable operation at −20 °C are reported as well as the system behaviour during long-term at 40 °C. A simple thermal model of the stack is developed and validated, and accounts for heat losses by radiation and convection. Condensation of steam is addressed as well as reaction gas depletion. The stack is regarded as a uniform heat source. The electrochemical reaction is not resolved. General design rules for the cold start-up of a portable fuel-cell stack are deduced by the thermal model and are taken into consideration for the design. The model is used for a comparison between active-assisted cold start-up procedures with a passive cold start-up from temperatures below 0 °C. It is found that a passive cold start-up may not be the most efficient strategy. Additionally, the influence of different stack concepts on the start-up behaviour is analysed by the thermal model. Three power classes of PEMFC stacks are compared: a Ballard Mk902 module for automotive applications with 85 kW, the forerunner stack Ballard Mk5 (5 kW) for medium power applications, and the developed OutdoorFC stack (30 W), for portable applications.

Keywords: Proton exchange membrane fuel-cell system; Outdoor application; Cold-start; Modelling; Portable; Automotive

1. Introduction

Portable applications are considered to be a very promising field for proton exchange membrane fuel cells (PEMFCs). Flexibility in design due to the separation of energy-storage and energy-conversion functions, potentially longer operation time, and a lower break-even cost point are seen as major advantages. For portable applications, the current price per kW is estimated by the US. Department of Energy to be US$ 5000 kW^{-1}, compared with a cost target of US$ 50 kW^{-1} [1] for automotive applications.

Portable PEMFC systems up to several 100 W operating under moderate indoor conditions have been successfully presented for mobile phones, laptop computers, digital camcorders and auxiliary power units [2]. A new challenge for portable fuel-cell systems is the ability to operate in a stable manner in outdoor conditions with ambient temperatures between −20 and 40 °C. Besides durability and maintenance, the cold-start ability is one of the hardest technical challenges for PEMFC systems.

Little data has been reported on the operational behaviour of PEMFCs below 0 °C, especially on cold start-up problems. Datta et al. [3] reported on a successful cold start-up and operation of a 500-W PEMFC system at the Antarctic for 10 days at −35 °C, but detailed data for the system control during start-up was not given. A 50-W fuel-cell system was operated for 1 h at −42 °C by Cargnelli et al. [4]. A catalytic burner was used to assist cold start-up.

Often problems occur with the peripheral components in the system. Freezing of excess water forced Chu et al. [5] to stop their fuel system after 9 h of operation at −10 °C, details of the system were not given. Ice formation within the fuel-cell stack is one the most relevant problems during a cold start-up. In the worst case, freezing of product water could lead to a blockage of the porous structures in the gas-diffusion layer (GDL) as found

* Corresponding author. Tel.: +49 7614588 5432; fax: +49 7614588 9432.
E-mail address: michael.oszcipok@ise.fraunhofer.de (M. Oszcipok).

0378-7753/$ – see front matter © 2006 Elsevier B.V. All rights reserved.
doi:10.1016/j.jpowsour.2006.01.005

Nomenclature

A_{front}	stack surface exposed to the forced convection (m^2)
A_{ppd}	perpendicular stack surface (m^2)
A_{Stack}	stack surface (m^2)
$c_{p,Stack}$	specific heat capacity of stack ($kJ\,kg^{-1}\,K^{-1}$)
FC	fuel cell
GDL	gas diffusion layer
$h_{i,in}$	enthalpy of entering species ($kJ\,kg^{-1}$)
$h_{i,in}$	enthalpy of leaving species ($kJ\,kg^{-1}$)
h_{Stack}	hight of stack (m)
l_{Stack}	length of stack (m)
m_{Stack}	mass of stack (kg)
MEA	membrane electrode assembly
n_{cell}	number of cells
PEM	polymer electrolyte membrane
$P_{nominal}$	nominal stack power (kW)
$\dot{Q}_{act}$	heat generated by active methods (W)
$\dot{Q}_{forced}$	heat loss by forced convection (W)
$\dot{Q}_{free}$	heat loss by free convection (W)
$\dot{Q}_{rad}$	heat loss by radiation (W)
$\dot{Q}_{th}$	heat generated by fuel-cell operation (W)
T_{amb}	ambient temperature (K)
T_{Stack}	stack temperature (K)
w_{Stack}	width of stack (m)

Greek symbols

α_{forced}	heat transfer coefficient for forced convection ($W\,m^{-2}\,K^{-1}$)
α_{free}	heat transfer coefficient for free convection ($W\,m^{-2}\,K^{-1}$)
σ_{12}	radiation exchange constant ($W\,m^2\,K^{-1}$)
χ	ratio electrochemical surface to thermal mass ($cm^2\,K\,kJ^{-1}$)

by Weisbrod et al. [6]. During isothermal, single-cell experiments, freezing processes in the electrode are associated with a reduction of reaction surface as found in [7,8]. The volume expansion during the phase change of water from liquid state to ice can lead to destruction and serious degradation of the porous catalyst layers. During thermal cycling of the PEMFC from −10 to 80 °C, Cho et al. [9] observed, by means of cyclic voltammetry, a significant loss of electrochemical active surface. While the porous structure of the catalyst layer is highly endangered by ice formation, the function of the polymer electrolyte membrane appears not to be strongly affected. For dry Nafion membranes, McDonald et al. [10] reported a reduction of the mechanical properties after 385 freeze–thaw cycles from −40 and 80 °C. Well humidified membranes exhibited no changes and the functionality was not affected.

To avoid degradation caused by cold start-up, several shut-down strategies are common. Most often gas purging procedures are applied when the fuel-cell stack is still at elevated temperatures. With this approach, residual water in the flow field and the porous components can be driven out [11–13]. Another way to prevent freezing of water in the stack is to use anti-freezing solutions like alcohol to flood the cell before freezing [14], or to fill the endangered small pores with inert liquids [15].

Different methods can be used for cold start-up. From a system aspect, the most simple is a passive method. This means that only the irreversible heat losses of the fuel-cell stack during operation are used for heating. Here, it must be considered that the interior heats up much faster than the outer regions like the end-plates as modelled in [16]. Cell-reversal effects have also to be taken into account, they give rise to channel blocking with ice.

For a fast system start, it could be beneficial to use additional heating for the stack. This could be done passively as reported in [17] where a functional coating of the flow-field enables an exothermic reaction with product water to heat up the bipolar plate. Active methods like heating via the cooling loop of the fuel-cell have been proposed in [13]. Several other methods, such as the use of catalytic combustion of hydrogen/oxygen mixtures in the fuel-cell stack or the use of electric heatings, are summarised in [18].

In this study, a 30-W portable fuel system that is able to operate between −20 and 40 °C is described. Start-up and shut-down at sub-zero temperatures is reported. By comparison of different fuel-cell stack concepts using a thermal stack model, key design parameters for sub-zero operation are elucidated.

2. Modelling of passive cold-start of fuel-cell stacks

During a passive cold start-up, the PEMFC stack is heated by its own thermal losses from irreversibilities during operation. In this approach, all peripheral components that are necessary to enable the electrochemical reaction, e.g., pumps and valves for the reactant supply, have to be operated. By contrast, during an active cold-start, the fuel-cell stack heating can be supported by other methods such as catalytic combustion.

To analyse the theoretical capability of different cold start-up strategies to heat up only the fuel-cell stack, a simple thermal model has been developed.

2.1. Model description

The fuel-cell stack is regarded as a uniform heat source with a thermal heating power $\dot{Q}_{th}$. For active cold start-up, heat can be generated as $\dot{Q}_{act}$. The enthalpy balance for the gas and water streams is included and condensation of steam is also addressed. Implemented heat sinks are the losses by radiation $\dot{Q}_{rad}$ and losses by free convection $\dot{Q}_{free}$ and forced convection $\dot{Q}_{forced}$.

The radiation losses are calculated by Eq. (1), i.e.,

$$\dot{Q}_{rad} = \sigma_{12} A_{Stack} \left(T_{Stack}^4 - T_{amb}^4 \right). \quad (1)$$

Here, σ_{12} denotes the radiation exchange constant and A_{Stack} is the stack surface exchanges radiation with the environment. All external surfaces of the stacks are considered.

The free convective losses are included in Eq. (2), i.e.,

$$\dot{Q}_{\text{free}} = \alpha_{\text{free}} A_{\text{ppd}} (T_{\text{amb}} - T_{\text{Stack}}) \quad (2)$$

α_{free} is the heat-transfer coefficient for free convection and A_{ppd} as the perpendicular stack surface. The forced convection losses are calculated with:

$$\dot{Q}_{\text{forced}} = \alpha_{\text{forced}} A_{\text{front}} (T_{\text{amb}} - T_{\text{Stack}}) \quad (3)$$

A_{front} is the stack surface which is exposed to the forced convection.

All these heat sinks are summarised as the heat loss $\dot{Q}_{\text{loss}}$. Consequently, the time-dependent temperature change of the fuel-cell stack could be expressed by an energy balance, i.e.,

$$m_{\text{Stack}} c_{\text{p,Stack}} \frac{\mathrm{d}T_{\text{Stack}}}{\mathrm{d}t} = \sum_i \dot{m}_{i,\text{in}} h_{i,\text{in}} + \sum_i \dot{m}_{i,\text{out}} h_{i,\text{out}} + \dot{Q}_{\text{loss}} + \dot{Q}_{\text{th}} \quad (4)$$

This differential equation can be solved analytical by the developed thermal stack model. Here, m_{Stack} is the mass and $c_{\text{p,Stack}}$ is the specific heat capacity of the stack. Comparable thermal models for fuel cells are also used in [18–20].

2.2. Model evaluation

The thermal model is evaluated with passive cold start-up measurements of portable fuel-cell stacks in a climatic chamber. The forced convection velocity from the climatic chamber circulation fan is 1.6 ms^{-1}. In Fig. 1 a passive start-up of a 6-cell stack is shown. After 4 min, the average single cell voltage is ~0.55 V at a current of 4 A. Within 28 min, the stack temperature increases from −10 to 26 °C. Simulation of the stack temperature with the same input parameters shows a good correlation with the experimental values. The evaluated thermal stack model can be used to develop basic design rules for cold start-up of the fuel-cell stack.

2.3. Stack heat capacity

The heat capacity of the fuel-cell stack has a very strong influence on the cold start-up velocity, as indicated in Fig. 2. Here, a simulation of the increase in stack temperature is shown.

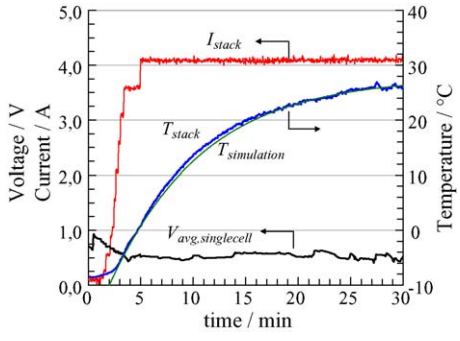

Fig. 1. Passive cold start-up of 6-cell fuel cell stack from −90 °C and simulation of the stack temperature.

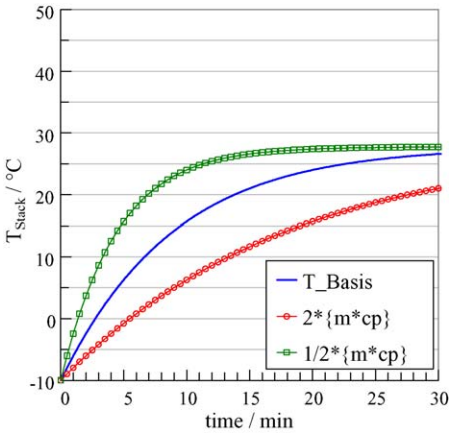

Fig. 2. Heat capacity has a strong influence on the velocity of cold start-up of fuel-cell stacks.

The heat capacity was varied using the model parameters from Fig. 1 for comparison (T_{Basis}). The mass of the fuel-cell stack is 0.4 kg with a specific heat capacity of 0.8 $\text{kJ kg}^{-1}\,\text{K}^{-1}$.

The heat capacity is a function of mass. As shown in Fig. 2, when the mass is doubled it takes 5 min to reach 0 °C. For example, when the mass is halved, it takes 1.4 min. This implies that lightweight materials should be used for the fuel-cell stack, such as thin, metallic bipolar plates instead of graphite plates.

2.4. Stack cell number

The influence of end-plates on the cold start-up behaviour is not negligible, as Fig. 3 indicates. The more cells that are included in a stack, the faster is the cold start-up. For the simulation, the number of cells is doubled/halved. The evaluation stack comprised of six cells.

2.5. Ambient temperature

The influence of ambient temperature on the cold start-up is significant. Simulations are conduced for varying external temperature between −20 and −5 °C. The results are shown in Fig. 4. The simulation demonstrates that it takes only 1.2 min

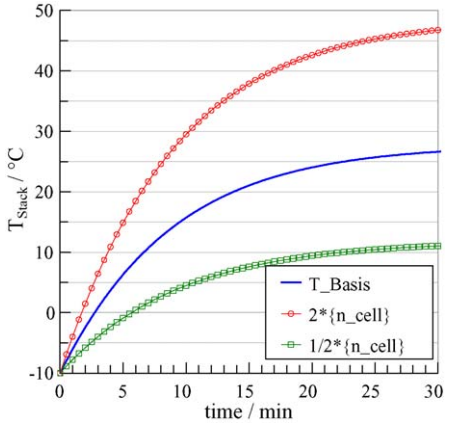

Fig. 3. The higher the cell number, the faster is the increase in temperature.

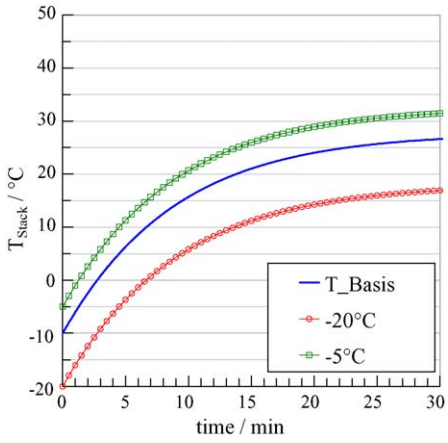

Fig. 4. Ambient temperature influence the cold start-up.

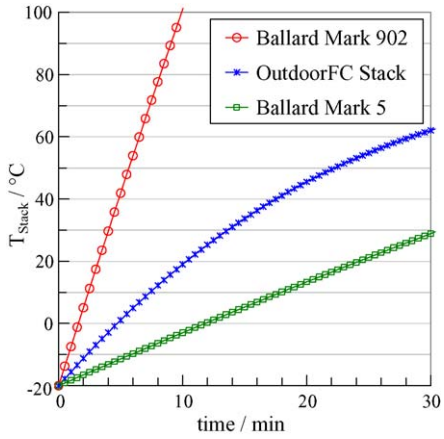

Fig. 5. Passive cold start-up of different fuel-cell stacks.

to increase the stack temperature from −5 to 0 °C. The time consumptions for the start-up from −20 to 0 °C takes 6.6 min.

2.6. Theoretical comparison of different stack concepts

The velocity of passive cold start-up of a fuel-cell stack depends strongly on the thermal heat generated in the stack. Different designs of stack have a strong impact on the cold-start ability. To determine which design parameters are important for cold start, three different stack concepts from different power classes were compared using the thermal model. The stacks are a 85-kW Ballard Mark 902 module for automotive applications, its forerunner model the 5-kW Ballard Mark 5 stack, and the portable 30-W OutdoorFC stack. The parameters used for thermal simulation are summarized in Table 1. The following assumptions were made.

- Each single cell has the same initial performance, i.e., 0.125 A cm^{-2} at 0.5 V. In this case, all stacks produce the same specific heat. This performance data is realistic for the portable OutdoorFC stack at −20 °C. It is assumed that the Ballard stacks have better performance at low temperature, but detailed data could not be found in the literature. Therefore, the same performance as measured for the OutdoorFC stack is assumed.
- The ambient temperature is −20 °C the gas pressures are 1.013×10^5 Pa and the air entering the stack is fully humidified.
- The stacks are operated with a gas stoichometry of 1.5 for hydrogen and 2.0 for air.
- Heat losses by forced convection are excluded.
- All stacks have the same specific heat capacity of 0.8 kJ kg^{-1} K^{-1}. A comparable value can be found in [19] for the Ballard Mark 5 stack. Experimental determination of the specific heat capacity of the OutdoorFC stacks confirmed this assumption. For the current generation of fuel-cell stacks, the bipolar plates are generally made of graphite-based materials, so this assumption was also made for the Mark 902 module.

Table 1
Stack data as used in thermal model for passive cold start-up simulation

Parameter	Unit	FhG ISE OutdoorFC	Ballard Mark 5	Ballard Mark 902
A_{ec}	cm^2	33	232 [22]	300
m_{Stack}	kg	0.4	43	96
$m_{Stack} \cdot c_{p,Stack}$	kJ K^{-1}	0.32	35	76.8
l_{Stack}	m	0.100	0.21	0.805
w_{Stack}	m	0.060	0.21	0.375
h_{Stack}	m	0.036	0.38	0.25
n_{cell}	–	6	35	440 [23]
$P_{nominal}$	kW	0.03	5.0	85

Data for Ballard Mark 5 are taken from [19] and for Ballard Mark 902 from [21] unless otherwise noted.

The simulated temperature increase for the different fuel-cell stacks is shown Fig. 5. The Ballard Mark 902 module reaches 0°C within 1.5 min, followed by the OutdoorFC stack (5 min) and the Ballard Mark 5 stack (11.5 min). The reason for these performances is the that the ratio χ of the electrochemical reaction surface of the stack and its thermal mass is very different for each stack. The higher the value of χ the more thermal heat is produced per thermal mass. This can be deduced from the ratio of the active material utilization and the inactive area of the bipolar plate for each stack. The calculated values for each stack are given in Table 2.

2.7. Design rules for fuel-cell stacks: passive cold start-up

Key design rules for passive cold start-up can be elucidated using the stack model.

Table 2
Ratio (χ) of electrochemical active surface and thermal mass, and percentage use of active bipolar plate area

Ratio	Unit	FhG ISE OutdoorFC	Ballard Mark 5	Ballard Mark 902
χ	cm^2 K kJ^{-1}	619	232	1719
Used bipolar plate area	%	~70	~50	~80

- For a fast heat up, a high utilization of the bipolar plates for the electrochemical reaction must be achieved. By that more heat per thermal mass can be produced.
- The economic use of materials and lightweight construction speed start-up.
- The simulation shows that stacks with a higher number of cells are favourable because this reduces end-plate effects.

In contrast to large automotive fuel-cell modules, portable fuel-cell stacks do not easily fulfil these demands. Often, the number of cells to necessary meet the power requirements of the applications is low such that the impact of the end-plates on the thermal dynamics is high. Thus, alternative methods for portable fuel-cell stacks must be considered for cold start-up.

3. Analysis of active heating

To support the cold-start capability of portable fuel-cell systems, additional heating could be beneficial. The thermal mass of the end-plates and of the peripheral components (such as valves) must be taken into account. Most importantly the fuel-cell stack should be above 0 °C before start-up because of severe degradation effects, e.g. ice formation [9,14,24,8], cell reversals (which means a local electrolysis) and channel blockage [25] caused by freezing of water droplets.

Here, two alternative methods have been investigated to heat a fuel-cell stack above 0 °C. A prototype of a catalytic burner plate which can be integrated into the fuel-cell stack is developed. The plate consists of graphite with a milled channel structure. The platinum-coated channels can be purged with hydrogen and air can diffuse through the open end of the channel to combust with the hydrogen. A 10.7 W catalytic H_2 burner demonstrated this approach, but its efficiency was poor, i.e., 8.3% (higher heating value of hydrogen). Nevertheless, the results obtained by experiments were used in the thermal model to compare the efficiency of this catalytic burner for heating a fuel-cell stack. The second method considered was to heat up the stack with an electric heating foil. In preliminary experiments, such a foil was incorporated into a bipolar plate and several experiements to heat up a stack were performed. As the developed OutdoorFC system is a hybrid system with a battery, this method is well suited.

3.1. Efficiency analyses

With the thermal model, an efficiency analysis was undertaken to compare the energy consumption for a passive cold start-up with the above described active methods. For the analyses, the energy consumption of all peripheral components that are necessary during the heating phase are included. For the passive cold start-up, a thermal heat production of 11.4 W is assumed, which represents 50% efficiency of the fuel cell stack. For the comparison with an active electrical cold start-up, a heating power 11.3 W is assumed and the heating power of the catalytic burner plate was 10.7 W. The energy consumption of the described methods when heating up a 6-cell OutdoorFC fuel-cell stack from −20 °C to higher temperatures is shown in Fig. 6.

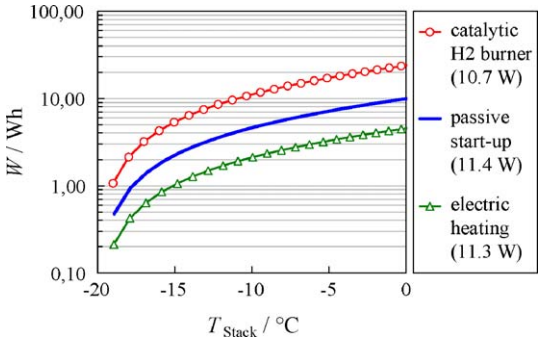

Fig. 6. Comparison of energy consumption between passive- and active-assisted cold start-up methods for fuel-cell stacks.

The energy consumption of the catalytic burner to heat up the stack to 0°C is more than 20 Wh, because of its low efficiency. While the start-up time for all three methods is comparable (about 10 min to reach 0 °C) the energy consumption differs strongly. The active electric cold start-up consumes 4.5 Wh (incl. a battery load efficiency of 85% and a fuel cell efficiency of 52%), and for the passive start-up 10 Wh are required. The reason is that during the latter start-up, all peripheral components have to be operated. Furthermore, the reaction gases carry heat out of the stack and this is not the case for the active-supported cold start-up. Consequently, the cold start option with a heating foil is preferred.

4. Outdoor fuel-cell system

4.1. Fuel-cell stack design

The OutdoorFC system has a 6-cell stack with an internal membrane humidity exchanger. For thermal management of the stack, cooling ribs are incorporated in the end-plates (aluminium). For cold start-up assistance, an electric heating foil is attached to the stack. Each bipolar plate is contacted with a pin to monitor single-cell voltages for system control. The OutdoorFC stack is shown in Fig. 7.

The bipolar plates are made of graphite with an active surface area of 30 cm^2 for each cell. The nominal power is 30 W and the

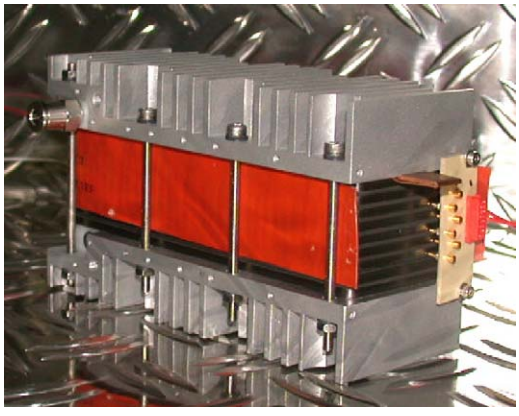

Fig. 7. Outdoor fuel-cell stack with internal humidiffier, electric heating, cooling ribs and single-cell contact pins for monitoring.

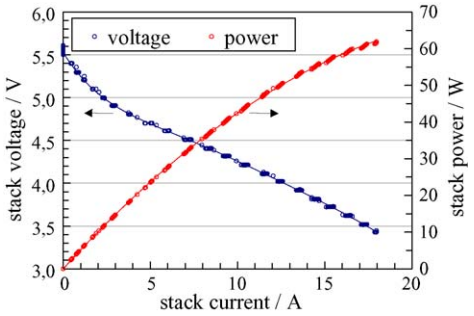

Fig. 8. Polarization curve and power for OutdoorFC stack measured during autonomous operation of the system at 60 °C stack temperature and 20 °C ambient temperature.

peak power is 65 W. A polarisation curve and the power characteristic of the OutdoorFC stack during autonomous system operation are presented in Fig. 8.

4.2. System design

The complete hydrogen/air operated system comprises the fuel-cell stack (see Fig. 7) as described, a Li-ion battery (6 Ah, 90 Wh), an anode and cathode pump, a water seperator with a purging valve and two inlet valves for the hydrogen supply. Single-cell voltages, current, power and several temperatures are monitored including the ambient temperature. To avoid overheating, the fuel-cell stack is equipped with a cooling fan that is turned on when the stack temperature increases 65 °C. A flow chart of the system is shown in Fig. 9.

To realize a fast start-up, the packaging of the peripheral components is critical. As can be seen in Fig. 10, the valves and the water separator are thermally connected to the fuel-cell stack to prevent freezing of water which could lead to blocking of the gas lines and therefore to a malfunction of the system. The system is thermally insulated and integrated into a housing with the dimensions 40 cm × 30 cm × 18 cm. The system output voltage is 12–16.5 V at a nominal power of 15 W and a peak power of 30 W. It can be operated between −20 and 40 °C ambient temperature.

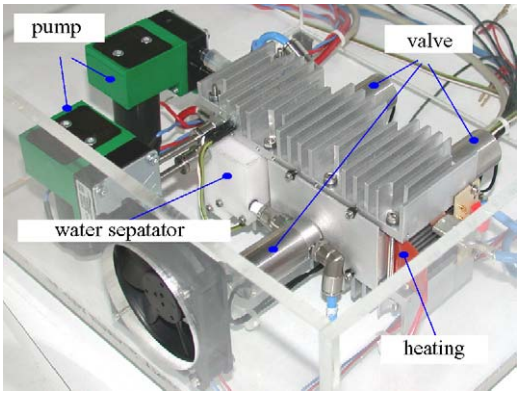

Fig. 10. System packaging in plexigals demonstration housing. Valves and water separator are thermally connected to stack and electrical heating foil.

4.3. System control

The system is completely digitally controlled by a printed-circuit board with an integrated Digital Signal Processor (DSP) that includes RS232 interfaces for data transfer. All relevant system data are monitored, namely, gas pressures, temperatures, single-cell voltages, and current. A low-volume boost converter has been developed by means of 180 °C phase delayed pulsing.

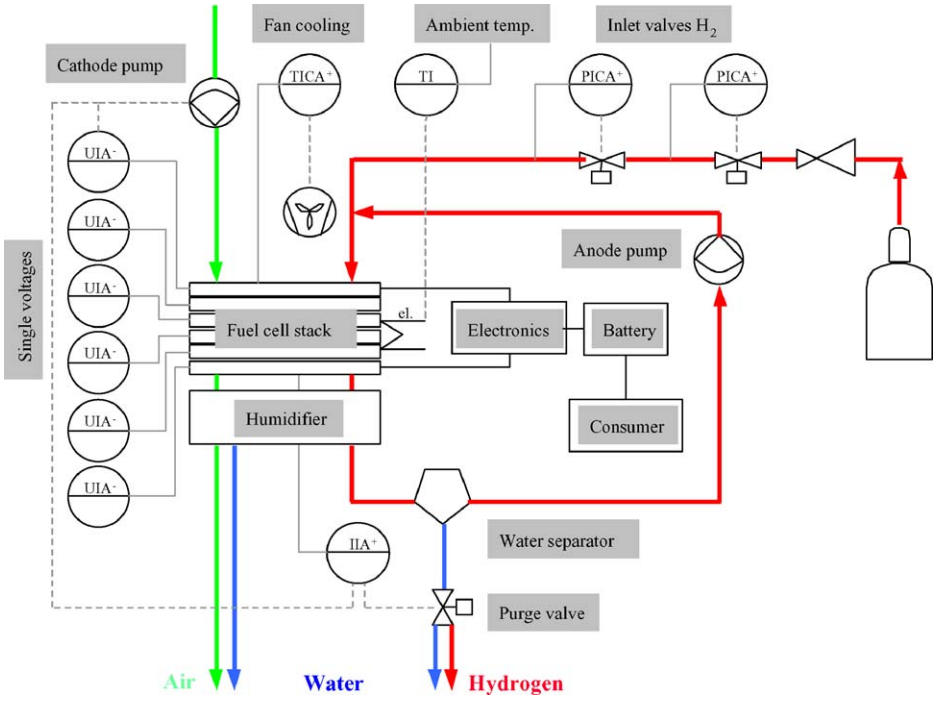

Fig. 9. Schematic sketch of the outdoor fuel-cell system.

Fig. 11. DSP controller for digital control of the fuel-cell system. All relevant system data can be displayed.

The highly efficient converter transforms the fuel-cell voltage to load a 4-cell Li-ion battery in a constant current–constant voltage mode (CC–CV). The battery temperature and single-cell voltages data also are monitored. The circuit board for the control of the system with the LCD-display and the DSP controller is shown in Fig. 11.

Before and during operation of the fuel-cell system, the electronic control conducts (i) extensive safety checks, e.g., the correct function of the valves, and (ii) system leakage tests to guarantee the correct operation of the system. The front panel includes switches for system on/off, consumer on/off, LCD display, start/stop, a RS 232 interface and a connection for the consumer.

4.4. Cold start-up

The most critical issue for use of the fuel-cell systems at ambient temperatures is the cold start-up. For portable fuel-cell systems where the thermal mass of the peripheral components is not negligible, a passive cold start-up is not reasonable. The system presented here is therefore heated (with a power of 30 W) before the fuel cell is started. When the temperature of the anode purging valve is 15 °C, it is found that the stack temperature has reached 0 °C. Hence, this was used as a control criteria. A repeated cold start procedure for the fuel-cell system from −20 °C is presented in Fig. 12.

After the stack is operated, it immediately delivers an output power of 30 W, and even more during dynamic operation.

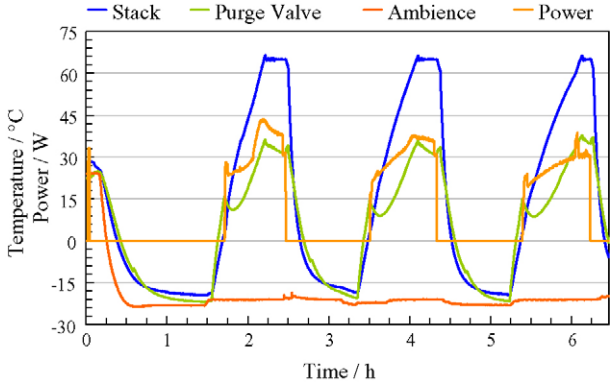

Fig. 12. Repeated cold start-ups from −20°C to operating temperature of the fuel-cell stack (65 °C).

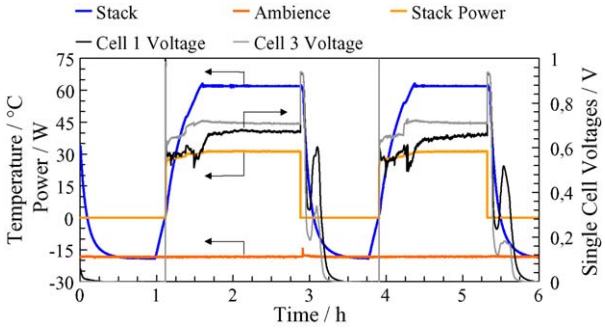

Fig. 13. Single-cell voltages are widely spread as long as the fuel-cell stack is below operating temperature.

For shut down, the stack was dried by reaction gases when still above 0 °C to blow out residual water from the flow-fields and the porous structures of both the gas diffusion layer and the catalyst layer. Even when the stack delivers 30 W after it has been started there is a significant single-cell voltage distribution. This is due to the development of temperature gradients in the stack, i.e., the temperature in the centre of the stack is higher than in the end cells. Due to thermal losses over the end-plates, flooding effects occur in the cells. The stack is operated at constant power and each cell delivers the same (stack) current and, therefore, the single-cell voltage is the varying operational parameter. This effect is clearly demonstrated in Fig. 13 which shows two cold start-ups and the single-cell voltages of cell 1, which is the upper end-cell adjacent to the end-plate and cell 3 which is a middle cell. After the stack temperature has reached 65 °C, the single cell voltages converge because the condensed water in the end-cells evaporates as the stack temperature approaches uniformity.

4.5. Long-term operation

To evaluate the outdoor capability of the developed system, it was operated in a climatic chamber between −20 and 40°C. The result of a long-term operation for 3 days at 40 °C is given in Fig. 14. The system delivered continuously 30 W. Even at −20 °C, the system shows constant performance, as indicated in Fig. 15. Over 3 days, the output power stayed stable. No freezing of water occurred in the fuel-cell stack, the critical purging valve of the anode loop or other peripheral components.

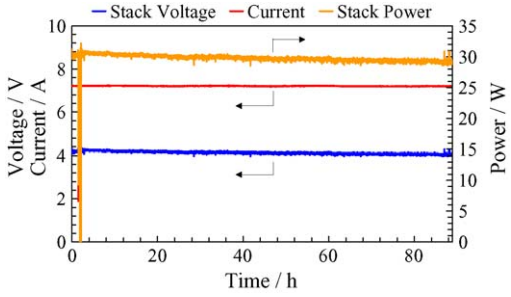

Fig. 14. Performance data during 3 days of operation of outdoor fuel-cell system in climatic chamber at 40 °C.

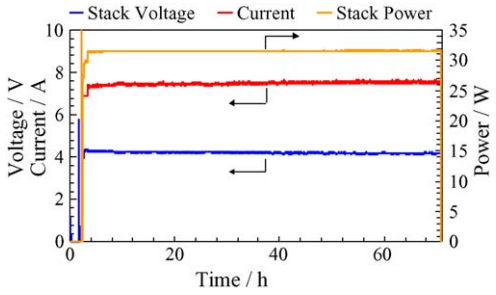

Fig. 15. Low-temperature operation at −20 °C for 3 days. The system delivers constant output power.

5. Conclusions

A series of key design rules for portable fuel-cell systems have been developed. This has been achieved with the aid of a thermal model. Using these design rules, it is found that a passive cold start-up of a portable system is not viable due to the thermal mass of the peripheral components and to end-plate losses. Consequently, active support to heat up the portable fuel-cell stack to 0 °C is recommended because of two considerations: (i) freezing of water can lead to severe degradation in the fuel cell (as confirmed by earlier studies [8]) and (ii) energy consumption could be lower for active heating systems than for passive ones. These theoretical results are used to design a 30-W fuel-cell system which is able to able to operate at −20 up to 40 °C. The cold start-up is assisted by electrical heating. Stable operation is demonstrated for more than 3 days in a climatic chamber at −20 °C without any freezing problems. Because the system is equipped with an internal membrane humidifier, operation at 40 °C is also successful. The autonomous operation is controlled by a digital signal processor which enables continuous outdoor operation of a hydrogen-powered, portable PEMFC system.

References

[1] J. Miliken Fuel Cells for Portable Power, http://www.eere.energy.gov/hydrogenandfuelcells/pdfs/fc_portable_power_ppt.pdf.
[2] K. Tüber, M. Zobel, H. Schmidt, C. Hebling, J. Power Sources 122 (2003) 1–8.
[3] B.K. Datta, G. Velayutham, A. Prassad Goud, J. Power Sources 106 (2002) 370–376.
[4] J. Cargnelli, P. Rivard, D. Frank, R.B. Gopal, Portable Fuel Cells Proc. (1999) 129–134.
[5] D. Chu, R. Jiang, K. Gardner, R. Jacobs, J. Schmidt, T. Quakenbush, J. Stephens, J. Power Sources 96 (2001) 174–178.
[6] K. Weisbrod, J. Hedstrom, J. Tafoya, R. Borup, M. Inbody, Fuel Cell Seminar 2000, Abstracts, Portland, 2000, pp. 90–93.
[7] F. Kagami, T. Ogawa, Y. Hishinuma, T. Chikahisa, Fuel Cell Seminar, Abstracts, 2002, pp. 239–242.
[8] M. Oszcipok, D. Riemann, U. Kronenwett, M. Kreideweis, M. Zedda, J. Power Sources 145 (2005) 407–415.
[9] E. Cho, J.-J. Ko, H.Y. Ha, S.-A. Hong, J. Electrochem. Soc. 150 (2003) A1667–A1670.
[10] R.C. McDonald, C.K. Mittelsteadit, E.L. Thompson, 2nd European PEFC Forum, 2003, Band Proceedings, vol. 1, Seiten, pp. 199–207.
[11] General Motors Corporation, Detroit MI (US), Freeze-protecting a fuel cell by vacuum drying, US Patent, 1999.
[12] Energy Partners, L.C. FL 33407 (US), Freeze tolerant fuel cell system and method, Patent, 1999.
[13] Ballard Power Systems Inc., Burnaby, British Columbia V5J5j9 (CA), Methods for improving the cold starting capability of an electrochemical fuel cell patent, 2000.
[14] E. Cho, J. Ko, H.Y. Ho, S. Hong, K. Lee, T. Lim, I. Oh, Effects of water removal on the performance degradation of PEMFCs repetitively brought to <0 °C, J. Electrochem. Soc. 151 (2004) 661–665.
[15] Ballard Power System Inc. Burnaby (CA), Method of reducing fuel cell performance degradation of an electrode comprising porous components, US Patent, 2001.
[16] M. Sundarsan, R.M. Moore, J. Power Sources 145 (2005) 534–545.
[17] DaimlerChrysler AG, 70567 Stuttgart (DE): Brenostoffzelle und Verfahren zum Kalstarten einer solchen Brennstaffzelle, Patent, 2003.
[18] M. Sundaresan, A. Thermal Model to Evaluate Sub-Freezing Startup for a Direct Hydrogen Hybrid Fuel Cell Vehicle Polymer http://www.its.ucdavis.edu/publications/2004/UCD-ITS-RR-04-05.pdf.
[19] J.C. Amphlett, R.F. Mann, B.A. Peppiey, P.R. Roberge, A. Rodrigues, J. Power Sources 61 (1996) 183–188.
[20] M. DeFrancesco, E. Arato, J. Power Sources 108 (2000) 41–52.
[21] S. Kim, S. Shimpalee, J. Electrochem. Soc. 152 (2005) A1265–A1271.
[22] DaimlerCharysler Research & Technology, Stuttgart: Necar 5 fahrenmit methanol, brochure, 2000.
[23] Ballard Power System Inc: Mark 902 Product Data, 2003, www.ballard.com/be_a_customer/transportation/fuel_cell_modules/mark902.
[24] Y. Goo, J. Kim, Fuel cell seminar Abstracts, pp. 117–120.
[25] A. Taniguchi, T. Akita, K.Y. Asuda, Y. Miyazaki, J. Power Sources 130 (2004) 42–49.